

~~approximate~~

~~add after full page~~ ~~This is a nucleus.~~  
~~From bare to full halo~~  
~~Hawking~~

structure with transfer

## Chapter 6

# Nuclear Structure with two-nucleon transfer

~~one- and~~

~~one- and~~

~~exotic halo nuclei  
( $^{11}\text{Be}$ ,  $^{11}\text{Li}$ )~~

In what follows, we apply the formalism worked out in the previous chapter with the help of software developed to calculate absolute two-particle transfer differential cross sections, associated with reactions induced by both light and heavy ions (cf. App. 6.D COOPER, ONE). A number of examples are treated with special detail. Namely, two-particle transfer in light pairing vibrational nuclei, including the halo unstable nucleus  $^{11}\text{Li}$ , in superfluid medium heavy nuclei lying along the stability valley (Sn-isotopes) and in heavy closed shell systems (Pb). In this last case both for light and heavy ion projectiles.

### 6.1 The $^1\text{H}(^{11}\text{Li}, ^9\text{Li})^3\text{H}$ reaction: evidence for phonon mediated pairing

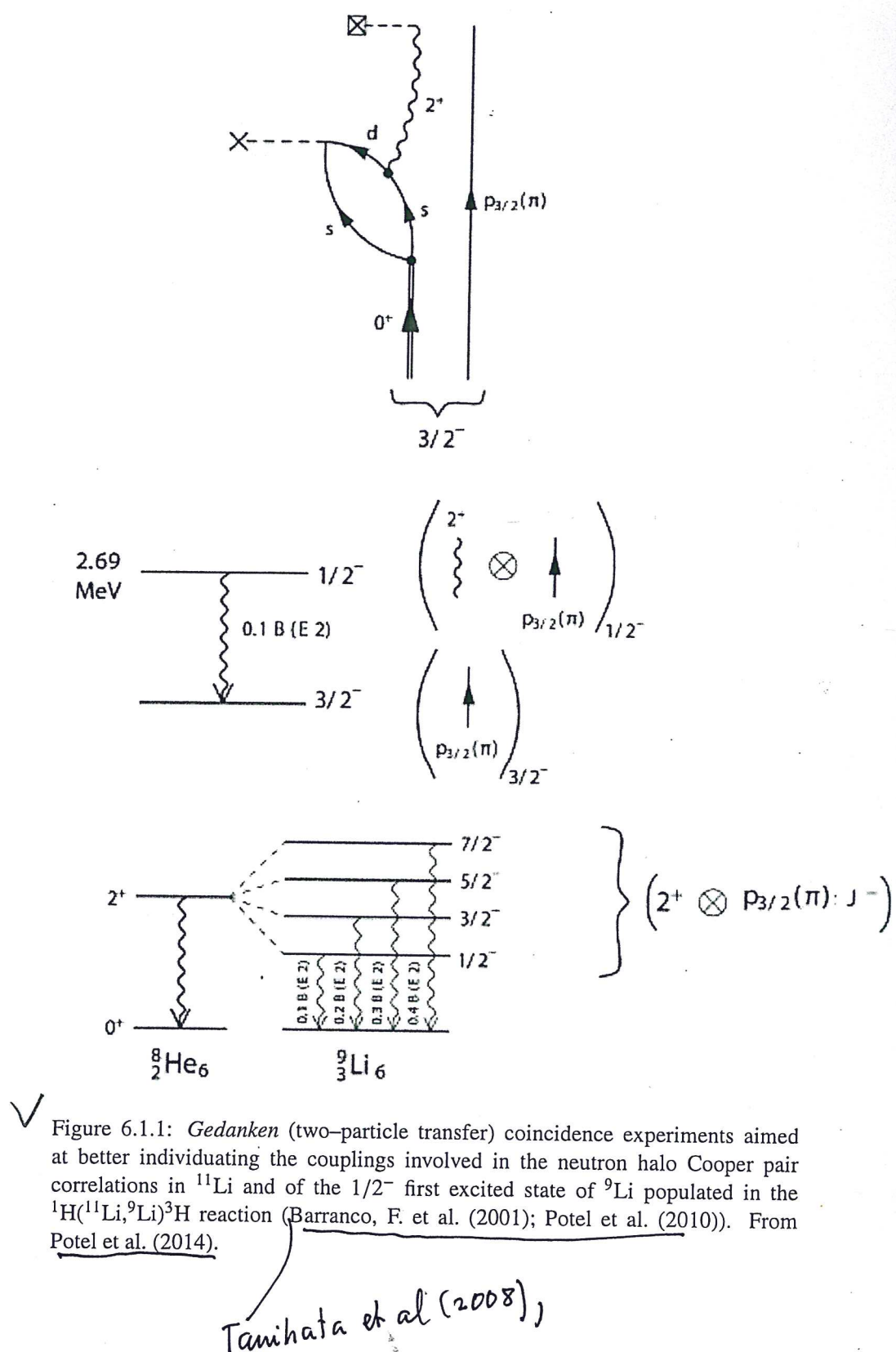
We start by discussing the analysis of the two-neutron pickup reaction  $^1\text{H}(^{11}\text{Li}, ^9\text{Li})^3\text{H}$  (Tanihata, I. et al., 2008). Particular attention is paid to the excitation of the  $1/2^-$  first excited state of  $^{9}\text{Li}$  lying at 2.69 MeV (cf. Figs. 6.1.1 and 6.1.2). To assess the direct character of the  $1/2^-$  excitation process, the importance of inelastic (cf. Apéndice 1E de la introducción inelastic scattering) and knockout (cf. Ch. 4) channels were considered and found to be small (see App. 6.B). The results thus provide evidence for a new mechanism of pairing correlations in nuclei: ~~pigmy resonance mediated pairing interaction~~ (Barranco, F. et al. (2001), see also App. 6.A), which strongly renormalizes the bare,  $NN^{-1}S_0$  interaction (Potel et al., 2010). This is but a particular embodiment of phonon mediated pairing interaction found throughout in nuclei (e.g. Barranco et al. (1999); Gori et al. (2004) cf. also Brink, D. and Broglia (2005)). The main difference between light halo exotic nuclei and medium heavy superfluid nuclei lying along the valley of stability is the role fluctuations play in dressing particles (quasiparticles) and in renormalizing their properties (mass, charge, etc.) and their interactions. In fact, in the case of e.g. Sn

\*)

379

\*\*) Barranco et al. 2001; Potel et al. (2010)

\*\*\*)



isotopes, mean field effects are dominant, while in the case of halo exotic nuclei renormalization effects can be as large as mean field ones.

### 6.1.1 Structure

Within the scenario presented in Chapter 2 (App. 2.6) and Chapter 4 (Sect. 4.2.2) the wavefunction describing the structure of the halo neutrons in the ground state of  $^{11}\text{Li}$  (the  $p_{3/2}$  proton being assumed to act only as a spectator) can be written as

$$|0\rangle_v = |0\rangle + \alpha|(p_{1/2}, s_{1/2})_{1^-} \otimes 1^-; 0\rangle + \beta|(s_{1/2}, d_{5/2})_{2^+} \otimes 2^+; 0\rangle, \quad (6.1.1)$$

with

$$\alpha = 0.7, \quad \text{and} \quad \beta = 0.1, \quad (6.1.2)$$

and

$$|0\rangle = 0.45|s_{1/2}^2(0)\rangle + 0.55|p_{1/2}^2(0)\rangle + 0.04|d_{5/2}^2(0)\rangle, \quad (6.1.3)$$

$|1^-\rangle$  and  $|2^+\rangle$  being the (RPA) states describing the dipole pigmy resonance of  $^{11}\text{Li}$  and the quadrupole vibration of the core. While these states are virtual excitations which, exchanged between the two neutrons bind them to the Fermi surface provided by the  $^9\text{Li}$  core, they can be forced to become real with the help of the specific probe of Cooper pairs in nuclei, namely two-particle transfer reactions (Figs. 6.1.2 and 6.1.3).

$^{11}\text{Li}(p, t)^9\text{Li}$												
	$V$	$W$	$V_{so}$	$W_d$	$r_1$	$a_1$	$r_2$	$a_2$	$r_3$	$a_3$	$r_4$	$a_4$
$p, ^{11}\text{Li}^d)$	63.62	0.33	5.69	8.9	1.12	0.68	1.12	0.52	0.89	0.59	1.31	0.52
$d, ^{10}\text{Li}^b)$	90.76	1.6	3.56	10.58	1.15	0.75	1.35	0.64	0.97	1.01	1.4	0.66
$t, ^9\text{Li}^c)$	152.47	12.59	1.9	12.08	1.04	0.72	1.23	0.72	0.53	0.24	1.03	0.83

Table 6.1.1: Optical potentials (cf. Tanihata, I. et al. (2008)) used in the calculation of the absolute differential cross sections displayed in Fig. 6.1.3.

We are then in presence of a paradigmatic nuclear embodiment of Cooper's model which is at the basis of BCS theory: a single weakly bound neutron pair on top of the Fermi surface of the  $^9\text{Li}$  core. But the analogy goes beyond these aspects, and covers also the very nature of the interaction acting between Cooper pair partners. Due to the the high polarizability of the system under study and of the small overlap of halo and core single particle wavefunctions, most of the Cooper pair correlation energy stems, according to NFT, from the exchange of collective vibrations, the role of the strongly screened bare interaction being, in this case, minor and subcritical (see App. 2.6). In other words, we are in the presence of a new realization of Cooper's model in which a totally novel Bardeen-Pines-Fröhlich-like phonon induced interaction is generated by a self induced collective vibration of the nuclear medium. In connection with (6.1.1), it is revealing that,

Sect.

~~moving  $^{11}\text{Be}$  to the present  
Ch. is OK  
the old number  
p. 266~~

~~Hawthorn  
2011~~

Summing up, virtual quadrupole vibrations of  ${}^8\text{He}$ , in its process of propagating from one partner of the halo neutron Cooper pair of  ${}^{11}\text{Li}$ , or to dress one of the partners has been caught in the act by the external pair transfer field produced by the ISAAC-2 facility at TRIUMF, forced to become a real final state and to bring this information to the active target detector MAYA.

The results →

the two final states excited in the inverse kinematics, two-neutron pick up reaction  ${}^1\text{H}({}^{11}\text{Li}, {}^9\text{Li}){}^3\text{H}$  are, the  $|3/2^-, \text{gs}({}^9\text{Li})\rangle$  and the first excited  $|1/2^-, 2.69\text{MeV}\rangle$  level of  ${}^9\text{Li}$ . Tanihata, I. et al. (2008). In fact, the associated absolute differential cross sections probe, within the NFT scenario, the  $|0\rangle$  and the  $|(\text{gs}_{1/2}, d_{5/2})_2^+ \otimes 2^+; 0\rangle$  component of the Cooper pair wavefunction respectively, (Fig. 6.1.2) (also Figs 4.2.5 and 4.2.6; also Figs. 6.1.3 and 2.6.3 (B)). They were calculated making use of modified formfactors worked out (App. 6.C) making use of the spectroscopic amplitudes given in Eqs. (6.1.1–6.1.3) and of the optical potentials collected in Table 6.1.1. and are compared with the experimental findings in Fig. 6.1.3. Theory reproduces the absolute two-particle differential cross section within experimental errors. But, more important, it provides a general picture of the physics behind the workings of halo pair addition modes.

### 6.1.2 Reaction

first excited state of  ${}^9\text{Li}$

Because second order calculations of inelastic, break up and final state interaction channels, which in principle can provide alternative routes for the population of the  $|1/2^-, 2.69\text{MeV}\rangle$  (see Fig. 6.B.1) state to that predicted by the wavefunction (6.1.1) ( $\beta$  component), lead to absolute cross sections which are smaller by few orders of magnitude than that shown in Fig. 6.1.3 (see Figs. 6.B.2, 6.B.3, as well as Table 6.B.1, Potel et al. (2010)), one can posit that quadrupole core polarization effects in  $|\text{gs}({}^{11}\text{Li})\rangle$  is essential to account for the observation of the  $|1/2^-, 2.69\text{ MeV}\rangle$  state, thus providing direct evidence for phonon mediated pairing in nuclei.

The reason why in the case of  ${}^{11}\text{Li}$  evidence for phonon mediated pairing is, arguably, inescapable, is connected with the fact that reaching the limits of stability associated with drip line nuclei, the system also reaches to situations in which medium polarization effects become overwhelming. In fact, one is, in such cases confronted with elementary modes of nuclear excitation in which dynamic fluctuation effects are as important as static, mean field effects. Within this context we refer to parity inversion (cf. Figs. 2.6.3 and 4.2.4). Nuclear Field Theory, within the Bloch–Horowitz (Dyson) set up, which allows one to sum to infinite order little convergent processes are specially suited to study these systems (cf. e.g. Barranco, F. et al. (2001) and Gori et al. (2004)). From these studies it emerges a possible new elementary mode of excitation, namely pair addition halo vibration, of which  $|\text{gs}({}^{11}\text{Li})\rangle$  state is a concrete embodiment. They are associated with a novel mechanism for stabilizing Cooper pairs, which arises from a (dynamical) breakup of gauge invariance (App 6.A). Their most distinctive feature, namely that of carrying on top of it a (dipole) pigmy resonance at a relative excitation energy of about 1 MeV, a necessary although not sufficient condition for this new mode to exist, can be instrumental for its characterization. While in the case of Li it constitutes the ground state, in other nuclei it may be an excited state which could be observed in a combined  $L = 0$ , and  $L = 1$ , two-particle transfer reaction to excited states, or in terms of  $E1$  decay of the pigmy resonance built on top of it. Within this context, it is an open question whether one could expect to find a realization of such a halo

\*) Tanihata et al (2008)

\*\*) ↗

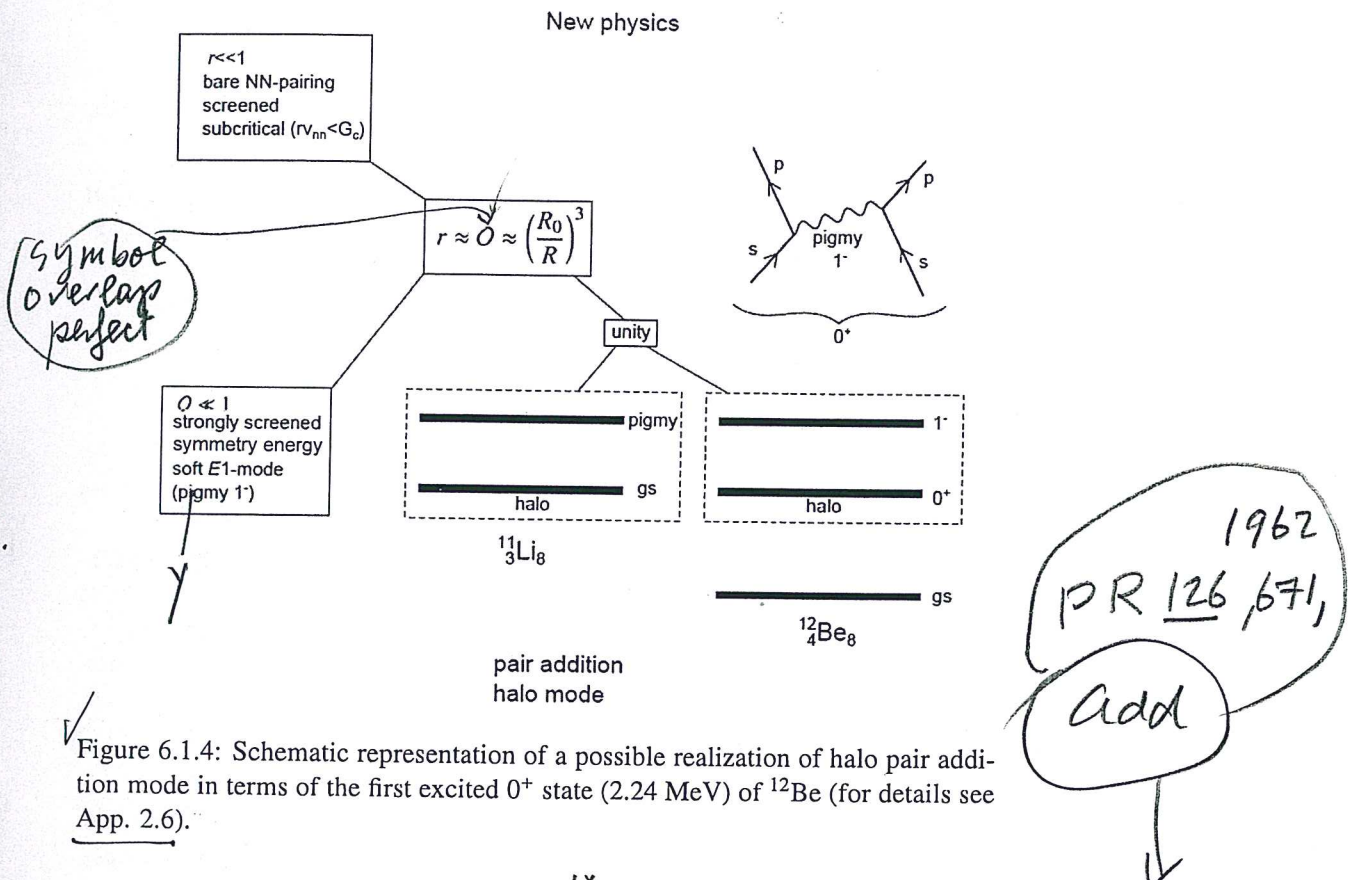


Figure 6.1.4: Schematic representation of a possible realization of halo pair addition mode in terms of the first excited  $0^+$  state (2.24 MeV) of  $^{12}\text{Be}$  (for details see App. 2.6).

pair addition mode in, for example, the first excited state of  $^{12}\text{Be}$  (see Fig. 6.1.4).

Pairing elementary modes of excitation based on  $s_{1/2}$  and  $p_{1/2}$  states at threshold have been found to lead, within the framework of a bare, short range, pairing interaction scheme to halo anti-pairing effects (cf. Bennaceur, K. et al. (2000), cf. also Hamamoto and Mottelson (2003), Hamamoto, I. and Mottelson (2004)). The fact that the separation energy of the halo neutrons (halo Cooper pair) of  $^{11}\text{Li}(\text{gs})$  is  $\approx 400\text{keV}$ , testifies to the fact that the anti-halo pairing effect is, in this case, overwhelmed by (dynamical) medium polarization effects.

Within this context it is of notice that, again, the interweaving of the different elementary modes of nuclear excitation, pairing and pigmy resonances in the present case, condition reaction studies, let alone the possibility to study (pigmy) giant resonances built on excited states, and to provide a novel test of the Brink-Axel hypothesis which is at the basis of the statistical description of photon decay from hot (compound) nuclei (cf. Brink (1955); cf. also Bortignon, P.F. et al. (1998), Bertsch, G. F. and Broglia (1986) and references therein).

Before concluding this section we provide in Fig. 6.1.5 examples of pairing vibrational states based on  $^{9}_3\text{Li}_6$ ,  $^{10}_4\text{Be}_6$ ,  $^{48}_{20}\text{Ca}_{28}$  and  $^{208}_{82}\text{Pb}_{126}$ ,  $N = 6$ ,  $N = 28$

\*)

\*\*\*)

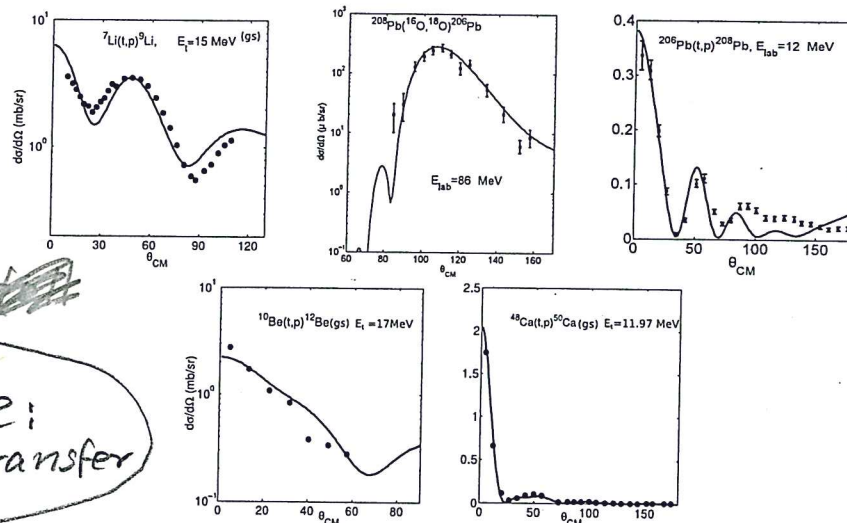


Figure 6.1.5: Absolute two-particle transfer differential cross sections for a number of reactions. Making use of spectroscopic amplitudes calculated as described in App. 2.5 in the particular case of  $N = 126$  (Pb),  $N = 48$  (Ca), and  $N = 6$  (Li,Be), of global optical parameters and of the software COOPER, the absolute differential cross sections were calculated and are displayed in comparison with the experimental data (after Potel, G. et al. (2013a)).

and  $N = 126$  neutron closed shell systems. The fact that among the  $(p,t)$  and  $(t,p)$  absolute differential cross sections one also finds the  $^{208}\text{Pb}(^{16}\text{O},^{18}\text{O})^{206}\text{Pb}(\text{gs})$  absolute differential cross section is in keeping with the fact that the formalism to treat both light and heavy ions two-nucleon transfer reactions and their connection is well known (cf. Broglia and Winther (2004), Bayman and Chen (1982) and Thompson (1988) and references therein) and rather homogeneous (cf. Potel, G. et al. (2013b)). Thus, it has been implemented in the software COOPER as a standard option (cf. App. 6.D).

## 6.2 Pairing rotational band with two-nucleon transfer: 6.3 Sn-isotopes

Nuclear superfluidity can be studied at profit in terms of the mean field, (cf. also Sect. 2.4.2) BCS diagonalization of the pairing Hamiltonian, namely,

$$H = H_{sp} + V_p, \quad (6.2.1)$$

where

$$H_{sp} = \sum_{\nu} (\epsilon_{\nu} - \lambda) a_{\nu}^{\dagger} a_{\nu}, \quad (6.2.2)$$

\*\*) Potel, G. et al (2013b)

while

$$V_p = -\Delta(P^+ + P) - \frac{\Delta^2}{G}, \quad (6.2.3)$$

and

$$\Delta = G\alpha_0, \quad (6.2.4)$$

is the pairing gap ( $\Delta \approx 12 \text{ MeV}/\sqrt{A}$ ),  $G$  ( $\approx 25 \text{ MeV}/A$ ) being the pairing coupling constant (Bohr, A., and Mottelson, 1975), and

$$P^+ = \sum_{v>0} P_v^+ = \sum_{v>0} a_v^+ a_{\bar{v}}^+, \quad (6.2.5)$$

$$P = \sum_{v>0} a_{\bar{v}} a_v, \quad (6.2.6)$$

are the pair addition and pair removal operators,  $a_v$  and  $a_v^+$  being single-particle creation and annihilation operators, ( $v\bar{v}$ ) labeling pairs of time reversal states.

The BCS ground state wavefunction describing the most favorable configuration of pairs to profit from the pairing interaction, can be written in terms of the product of the occupancy probabilities  $h_v$  for individual pairs,

$$|BCS\rangle = \prod_{v>0} ((1-h_v)^{1/2} + h_v^{1/2} a_v^+ a_{\bar{v}}^+) |0\rangle, \quad (6.2.7)$$

where  $|0\rangle$  is the fermion vacuum (Schrieffer (1964); Schrieffer, J. R. (1973)).

Superfluidity is tantamount to the existence of a finite average value of the operators (6.2.5), (6.2.6) in this state, that is, to a finite value of the order parameter

$$\alpha_0 = \langle BCS | P^+ | BCS \rangle = \langle BCS | P | BCS \rangle^*, \quad (6.2.8)$$

which is equivalent to Cooper pair condensation. In fact,  $\alpha_0$  gives a measure of the number of correlated pairs in the BCS ground state which in the nuclear case is few units ( $< 10$ ). While the pairing gap (6.2.4) is an important quantity relating theory with experiment,  $\alpha_0$  provides the specific measure of superfluidity. In fact, the matrix elements of the pairing interaction may vanish for specific regions of space, or in the case of specific pairs of time reversal orbits, but this does not necessarily imply a vanishing of the order parameter  $\alpha_0$ , nor the obliteration of superfluidity.

In keeping with the fact that Cooper pair tunneling is proportional to  $|\alpha_0|^2$ , this quantity plays also the role of a ( $L = 0$ ) two-nucleon transfer sum rule, sum rule which is essentially exhausted by the superfluid nuclear  $|BCS\rangle$  ground state (see Fig. 2.1.3).

### 6.2.1 Fluctuations

The BCS solution of the pairing Hamiltonian was recasted by Bogoliubov (1958) and Valatin (1958) in terms of quasiparticles.

$$\alpha_v^+ = U_v a_v^+ - V_v a_{\bar{v}}, \quad (6.2.9)$$

\*\*) Bogoliubov (1958), Valatin (1958);  
~~also~~ see also Bruek, D. and Broglia (2005) Appendix G.

linear transformation inducing the rotation in  $(a^+, a)$ -space which diagonalizes the Hamiltonian (6.2.1).

The variational parameters  $U_\nu, V_\nu$  appearing in the above relation indicate that  $a_\nu^+$  acting on  $|0\rangle$  creates a particle in the state  $|\nu\rangle$  which is empty with a probability  $U_\nu^2 (\equiv (1 - h_\nu) = (1 + (\epsilon_\nu - \lambda)/E_\nu)/2)$ , and annihilates a particle in the time reversal state  $|\bar{\nu}\rangle$  (creates a hole) which is occupied with probability  $V_\nu^2 (\equiv h_\nu = (1 - (\epsilon_\nu - \lambda)/E_\nu)/2)$ . Thus,

$$|BCS\rangle = \prod_{\nu>0} (U_\nu + V_\nu a_\nu^+ a_{\bar{\nu}}^+) |0\rangle, \quad (6.2.10)$$

is the quasiparticle vacuum, as  $|BCS\rangle \sim \prod_\nu \alpha_\nu |0\rangle$ , the order parameter being

$$\alpha_0 = \sum_{\nu>0} U_\nu V_\nu. \quad (6.2.11)$$

In Table 6.2.1 we collect the spectroscopic amplitudes associated with the reactions  $A^{+2}\text{Sn}(p,t)^A\text{Sn}$ , for  $A$  in the interval 112–126. Making use of these results and of global optical parameters (see Table 6.2.2), the absolute differential cross section  $A^{+2}\text{Sn}(p,t)^A\text{Sn}(\text{gs})$  were calculated. They are shown in Fig. 6.2.1 in comparison with the data.

### 6.2.2 Pairing rotations

	$^{112}\text{Sn}$	$^{114}\text{Sn}$	$^{116}\text{Sn}$	$^{118}\text{Sn}$	$^{120}\text{Sn}$	$^{122}\text{Sn}$	$^{124}\text{Sn}$
$1d_{5/2}$	0.664	0.594	0.393	0.471	0.439	0.394	0.352
$0g_{7/2}$	0.958	0.852	0.542	0.255	0.591	0.504	0.439
$2s_{1/2}$	0.446	0.477	0.442	0.487	0.451	0.413	0.364
$1d_{3/2}$	0.542	0.590	0.695	0.706	0.696	0.651	0.582
$0h_{11/2}$	0.686	0.720	1.062	0.969	1.095	1.175	1.222

Table 6.2.1: Two-nucleon transfer spectroscopic amplitudes  $\langle BCS(A)|P_\nu|BCS(A+2)\rangle = \sqrt{(2j_\nu + 1)/2} U_\nu(A) V_\nu(A+2)$ , associated with the reactions connecting the ground states (members of a pairing rotational band) of two superfluid Sn-nuclei  $A^{+2}\text{Sn}(p,t)^A\text{Sn}(\text{gs})$  (Potel, G. et al. (2013a)).

The phase of the ground state BCS wavefunction may be chosen so that  $U_\nu = |U_\nu| = U'_\nu$  is real and  $V_\nu = V'_\nu e^{2i\phi}$  ( $V'_\nu \equiv |V_\nu|$ ). Thus (Schrieffer, J. R., 1973),

$$\begin{aligned} \langle BCS(A)|P_\nu|BCS(A+2)\rangle &= \langle BCS(\phi)|\mathcal{K}|BCS(A+2)\rangle \\ &= \langle BCS(\phi)|\mathcal{K}'|BCS(A+2)\rangle = \prod_{\nu>0} (U'_\nu + V'_\nu a_\nu^{'+} a_{\bar{\nu}}^{'+}) |0\rangle = \prod_{\nu>0} (U'_\nu + V'_\nu a_\nu^{'+} a_{\bar{\nu}}^{'+}) |0\rangle \\ &= |BCS(\phi=0)\rangle_{\mathcal{K}'}, \end{aligned} \quad (6.2.12)$$

where  $a_\nu^{'+} = e^{-i\phi} a_\nu^+$  and  $a_{\bar{\nu}}^{'+} = e^{-i\phi} a_{\bar{\nu}}^+$ . This is in keeping with the fact that  $a_\nu^+$  and  $a_{\bar{\nu}}^+$  are single-particle creation operators which under gauge transformations (rotations in the 2D-gauge space of angle  $\phi$ ) induced by the operator  $G(\phi) = e^{-i\hat{N}(\phi)}$  and connecting the intrinsic and the laboratory frames of reference  $\mathcal{K}'$  and  $\mathcal{K}$  respectively, behave according to  $a_\nu^{'+} = G(\phi) a_\nu^+ G^{-1}(\phi) = e^{-i\phi} a_\nu^+$  and  $a_{\bar{\nu}}^{'+} = G(\phi) a_{\bar{\nu}}^+ G^{-1}(\phi) = e^{-i\phi} a_{\bar{\nu}}^+$ .

\* Schrieffer J.R., 1973

	${}^A\text{Sn}(p, t){}^{A-2}\text{Sn}$											
	$V$	$W$	$V_{so}$	$W_d$	$r_1$	$a_1$	$r_2$	$a_2$	$r_3$	$a_3$	$r_4$	$a_4$
$p, {}^A\text{Sn}^a)$	50	5	3	6	1.35	0.65	1.2	0.5	1.25	0.7	1.3	0.6
$d, {}^{A-1}\text{Sn}^b)$	78.53	12	3.62	10.5	1.1	0.6	1.3	0.5	0.97	0.9	1.3	0.61
$t, {}^{A-2}\text{Sn}^a)$	176	20	8	8	1.14	0.6	1.3	0.5	1.1	0.8	1.3	0.6

Table 6.2.2: Optical potentials used in the calculations of the absolute differential cross sections displayed in Fig. 6.2.1.

$e^{-i\phi}a_\nu^+$ , a consequence of the fact that  $\hat{N}$  is the number operator and that  $[\hat{N}, a_\nu^+] = a_\nu^+$ .

The fact that the mean field ground state ( $|BCS(\phi)\rangle_K$ ) is a product of operators - one for each pair state - acting on the vacuum, implies that (6.2.12) represents an ensemble of ground state wavefunctions averaged over systems with ...  $N-2, N, N+2$  ... even number of particles. In fact, (6.2.12) can also be written in the form

$$\begin{aligned} |BCS\rangle_K = (\Pi_{\nu>0} U'_\nu) (1 + \dots + \frac{e^{-(N-2)i\phi}}{(\frac{N-2}{2})!} \left( \sum_{\nu>0} c_\nu a_\nu^+ a_\nu^+ \right)^{\frac{N-2}{2}} + \frac{e^{-Ni\phi}}{(\frac{N}{2})!} \left( \sum_{\nu>0} c_\nu a_\nu^+ a_\nu^+ \right)^{\frac{N}{2}} \\ + \frac{e^{-(N+2)i\phi}}{(\frac{N+2}{2})!} \left( \sum_{\nu>0} c_\nu a_\nu^+ a_\nu^+ \right)^{\frac{N+2}{2}} + \dots) |0\rangle, \end{aligned} \quad (6.2.13)$$

where  $c_\nu = V'_\nu / U'_\nu$ .

Adjusting the Lagrange multiplier  $\lambda$  (chemical potential, see Eqs. (6.2.9, 6.2.10) and associated text), one can ensure that the mean number of fermions has the desired value  $N_0$ . Summing up, the BCS ground state is a wavepacket in the number of particles. In other words, it is a deformed state in gauge space defining a privileged orientation in this space, and thus an intrinsic coordinate system  $K'$  (Anderson, 1958; Bohr, 1964; Bès, D. R. and Broglia, 1966). The magnitude of this deformation is measured by  $\alpha_0$ , a quantity whose modulus squared value is connected with the absolute value of the two-nucleon transfer cross section. A further element, if it was still the need, which testifies that two-nucleon transfer is specific to probe pairing in nuclei.

### 6.2.3 Pairing vibrations in superfluid nuclei

All the above arguments, point to a static picture of nuclear superfluidity which results from BCS theory. This is quite natural, as one is dealing with a mean field approximation. The situation is radically changed taking into account the interaction acting among the Cooper pairs (quasiparticles) which has been neglected until now, that is the term  $-G(P^+ - \alpha_0)(P - \alpha_0)$  left out in the mean field (BCS) approximation leading to (6.2.3). This interaction can essentially be written as (for details

### 6.2.3 Structure-reaction stability of $\alpha_0$

Below we discuss

\*)

\*\*) ↘

footnote \*\*)  
p. 390

see e.g. Brink, D. and Broglia (2005) Apps. G, I and J and references therein)

$$H_{\text{residual}} = H'_p + H''_p, \quad (6.2.14)$$

where

$$H'_p = -\frac{G}{4} \left( \sum_{\nu>0} (U_\nu^2 - V_\nu^2)(P_\nu^+ + P_\nu^-) \right)^2, \quad (6.2.15)$$

and

$$H''_p = \frac{G}{4} \left( \sum_{\nu>0} (P^+ - P^-) \right)^2. \quad (6.2.16)$$

The term  $H'_p$  gives rise to vibrations of the pairing gap which (virtually) change particle number in  $\pm 2$  units. The energy of these pairing vibrations cannot be lower than  $2\Delta$ . They are, as a rule, little collective, corresponding essentially to almost pure two-quasiparticle excitations (see excited  $0^+$  states of Fig. 2.1.3).

The term  $H''_p$  leads to a solution of particular interest, displaying exactly zero energy, thus being degenerate with the ground state. The associated wavefunction is proportional to the particle number operator and thus to the gauge operator inducing an infinitesimal rotation in gauge space. The fluctuations associated with this zero frequency mode diverge, although the Hamiltonian defines a finite inertia. A proper inclusion of these fluctuations (of the orientation angle  $\phi$  in gauge space) restores gauge invariance in the  $|BCS(\phi)\rangle_K$  state leading to states with fixed particle number

$$|N_0\rangle \sim \int_0^{2\pi} d\phi e^{iN_0\phi} |BCS(\phi)\rangle_K \sim \left( \sum_{\nu>0} c_\nu a_\nu^+ a_\nu^- \right)^{N_0/2} |0\rangle. \quad (6.2.17)$$

These are the members of the pairing rotational band, e.g. the ground states of the superfluid Sn-isotope nuclei. These states provide the nuclear embodiment of Schrieffer's ensemble of ground state wavefunctions which is at the basis of the BCS theory of superconductivity. An example of such a rotational band is provided by the ground states of the Sn-isotopes (cf. Fig. 2.1.3). Making use of COOPER, namely of an implementation of two-nucleon transfer second order DWBA which includes successive and simultaneous transfer, properly corrected from non-orthogonality contributions, of the spectroscopic amplitudes collected in Table 6.2.1 (see also Table 2.4.1), and of global optical parameters from the literature (see Table 6.2.2), the two-nucleon transfer absolute differential cross sections associated with the Sn-isotopes rotational band have been calculated. They are compared with the experimental findings in Fig. 6.2.1 (cf. also Fig. 2.2.1 and Potel, G. et al. (2013a,b)).

Summing up, a collective solution always comes at frequency  $\nu = 0$ . Proper inclusion of the associated divergent ZPF of the  $\nu = 0$  modes restores symmetry by projecting the solution onto the laboratory frame of reference, where measurements can be carried out and thus, symmetries are to be respected. Within his context, it

\*)